Postprint of: Niedźwiecki M., Meller M. (2021) Active Suppression of Nonstationary Narrowband Acoustic Disturbances. In: Kulczycki P., Korbicz J., Kacprzyk J. (eds) Automatic Control, Robotics, and Information Processing. Studies in Systems, Decision and Control, vol 296. Springer, Cham. https://doi.org/10.1007/978-3-030-48587-0_26

Active Suppression of Nonstationary Narrowband Acoustic Disturbances

Maciej Niedźwiecki and Michał Meller

Abstract : In this chapter, a new approach to active narrowband noise control is presented. Narrowband acoustic noise may be generated, among others, by rotating parts of electro-mechanical devices, such as motors, turbines, compressors, or fans. Active noise control involves the generation of "antinoise" , i.e., the generation of a sound that has the same amplitude, but the opposite phase, as the unwanted noise, which causes them to interfere destructively, rather than constructively. In the range of low frequencies (below 1 kHz), the active approach is more effective than passive methods that employ dampers, barriers, absorbers, and other forms of acoustic isolation.

1 Introduction

One of the negative aspects of the growth of technology is the increase of various risk factors, such as acoustic noise. Long-term exposure to noise may cause fatigue, loss of focus and insomnia, or, in case of high levels of the noise, partial or total hearing loss.

Traditional methods of reducing acoustic noise rely on measures such as hearing protections, attenuators, dampeners, or acoustic isolators, among others. Such solutions, which can be referred to as passive, are most effective in the ranges of medium and high frequencies. Unfortunately, at low frequencies, the volume and mass of passive solutions grows substantially, which is a major drawback of this group of methods.

Recently, there has been a considerable growth in interest for active noise control (ANC). Active noise control methods rely on the phenomenon of destructive interference of acoustic waves. Without going into details, an ANC system generates an "antisound", i.e., an acoustic wave whose superposition with the undesired acoustic field results in the, typically local, cancellation of the latter. In contrast to passive methods, active noise control is most effective in the low-frequency range. This property stems from the fact that the volume of the space in which the cancel-

Maciej Niedźwiecki
Gdańsk University of Technology, Faculty of Electronics, Telecommunications and Informatics, Department of Automatic Control, Narutowicza 11/12, 80-233 Gdańsk, e-mail: maciekn@eti.pg.edu.pl; ORCID: https://orcid.org/0000-0002-8769-1259

Michał Meller
Gdańsk University of Technology, Faculty of Electronics, Telecommunications and Informatics, Department of Automatic Control, Narutowicza 11/12, 80-233 Gdańsk, e-mail: michal.meller@eti.pg.edu.pl; ORCID: https://orcid.org/0000-0001-5964-7085

lation takes place increases with the wavelengths of the interfering acoustic fields [33].

Fig. 1 depicts three basic configurations of ANC systems in the classical application of noise cancellation in an acoustic duct. The differences between the configurations include, among others, the controller's principle of operation, the number of sensors required in the system, and their placement in the duct. The elements common to all configurations are the noise source, the acoustic duct, a loudspeaker, and the measurement microphone, placed at the end of the duct, which senses the residual noise.

In the ANC systems literature, the undesired acoustic noise is typically referred to as the primary noise, and the fragment of the duct between the noise source and the measurement microphone is called the primary path. The loudspeaker that is placed inside the duct is the canceling loudspeaker. Its purpose is to generate an acoustic wave, called a secondary noise, that will cancel the primary noise. Consequently, the fragment of the duct between the loudspeaker and the measurement microphone is called the secondary path. Finally, the role of the measurement microphone is to sense the control results and to enable the computation of adjustments to the control signal.

Most ANC systems employ the so-called feedforward approach (Fig. 1a). Feedforward systems take advantage of the fact that sound travels at speeds that are many orders of magnitude slower than the propagation velocity of electrical signals. Using an additional microphone, typically placed close to the noise source, the so-called reference signal is collected. The reference signal carries the information about the primary noise ahead of time, in the sense that it reaches the controller well before the primary noise acoustic wave reaches the end of the duct. It follows that, by taking into account the transfer functions of the primary and the secondary paths, one may compute how to excite the loudspeaker to cancel the primary noise. An important feature of feedforward ANC systems is their capability to cancel wideband noise. On the other hand, to work effectively, feedforward systems require that the transfer delay of the primary path is longer than the time needed by the controller to compute the control signal. Moreover, the performance of feedforward ANC systems depends heavily on the quality of the reference signal or, more precisely, on the level of correlation between the reference signal and the primary noise [25].

The feedback configuration, depicted in Fig. 1b, is free of the above limitations. In this approach, the control signal is generated solely using the signal from the measurement microphone. Feedback systems, however, are capable of eliminating narrowband noise only, which stems from the fact that the computation of the control signal relies on predictions of the primary noise, which are accurate only for narrowband signals [73].

The hybrid configuration, shown in Fig. 1c, attempts to combine the advantages and, at the same time, to avoid the disadvantages of the above two approaches. This configuration employs both the feedforward and the feedback controllers, whose roles are to cancel the wideband and the narrowband components of the primary noise, respectively.

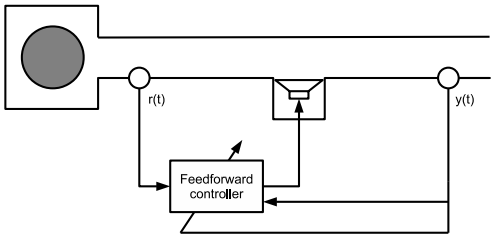

(a) Feedforward ANC system

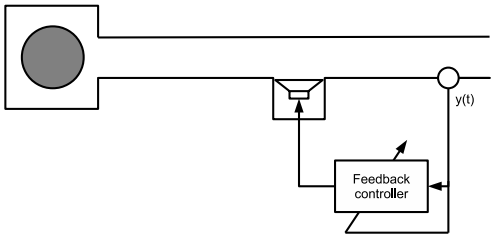

(b) Feedback ANC system

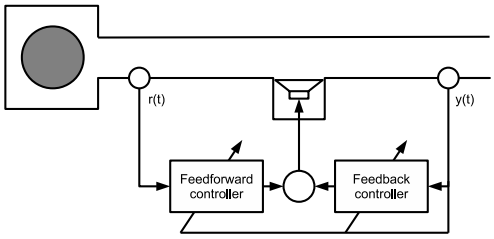

(c) Hybrid ANC system that combines feedforward and feedback approaches

Fig. 1 Typical configurations of active noise control systems in acoustic ducts.

The most popular control algorithm in active noise control is the FX-LMS filter [39]. The FX-LMS controller employs an adaptive finite impulse response (FIR) filter, whose coefficients are adjusted using a version of the least mean square (LMS) algorithm, modified so as to take into account the influence of the secondary path. The FX-LMS algorithm is suitable both for the feedforward [25] and the feedback configurations [33]. The relatively easy tuning and the variety of modifications, which are often heuristic [25], are only two of its numerous advantages. On the other hand, the FX-LMS controller is computationally complex, which stems from the large number of adjusted adaptive filter coefficients (typically between few hundreds and few thousands tapped delay line weights).

There exists several equivalents of the FX-LMS algorithm that employ the infinite impulse response (IIR) filters [12, 14, 16]. Remarkably, in active noise control systems, the primary reason to use the IIR filters is, rather unexpectedly, not the reduction of the computational complexity, but the elimination of the risk of the

adaptive controller destabilizing, related to the leakage of the canceling signal to the reference microphone [25]. However, the poles of the IIR filter might temporarily leave the unit disc during adaptation, which makes the issue of setting the initial values of the filter's coefficients the critical problem. The difficulty of ensuring safe operation of IIR filters is, likely, the reason of the dominance of the FX-LMS algorithm.

Several algorithms dedicated to the use of ANC systems that employ feedback were proposed as well. Despite their apparent differences, the basic principle underlying their operation is the same in all cases. Rejection of disturbances in feedback control systems requires high open loop gain at the frequencies that correspond to the spectral content of the disturbance [68]. Since the rejected disturbance signal might be nonstationary, i.e., the frequencies of its components might vary, the use of adaptive controllers is advised.

One may satisfy the above two requirements by combining a straightforward second order filter, whose poles are located at the unit circle, with a suitable frequency estimation mechanism, whose output serves to adapt the locations of the filter's poles. Among several advantages of this approach, its flexibility stands out as one of the most important. One is allowed to employ both parametric frequency estimators, based on a model of the disturbance [40, 64, 71], and nonparametric ones, such as FFT or subspace-based methods (e.g. classical MUSIC [66] and ESPRIT [65] algorithms). The controllers based on this approach were proposed in [3, 4, 20], among others.

The internal model principle (IMP) is another powerful framework for constructing feedback ANC controllers. The IMP principle states that a two degrees of freedom controller with transfer function $R(\zeta)/S(\zeta)$ (depending on the time domain, the symbol ζ corresponds to the complex variable s or z) ensures asymptotic cancellation of a disturbance $N(\zeta)/D(\zeta)$ if, and only if, a subset of the poles of the controller replicates the roots of the polynomial $D(\zeta)$, i.e., when $S(\zeta) = S'(\zeta)D(\zeta)$. IMP adaptive controllers may employ both indirect and direct adaptation mechanisms [1, 29]. In the first case, a model of the disturbance is estimated explicitly and the controller is synthesized by solving a Diophantine equation that includes the disturbance model [29]. In the direct approach, the controller is adapted without any intermediate steps, e.g., using the Youla-Kucera parametrization [67].

Note that each of the above referenced solutions requires the knowledge of the transfer function of the secondary path. There exist many applications where the plant may be regarded as stationary and its identification may be carried out once, typically in the open loop configuration. However, when the plant is subject to unpredictable changes, it is necessary to equip the controller with means to perform the identification on-line, without interrupting the operation of the ANC system.

The most popular solution of the problem of identifying a secondary path is the auxiliary noise approach, proposed in [15]. The method relies on introducing an additional signal, in the form of white noise, that excites the plant, to the control loop. The main disadvantage of such an approach is that the overall level of disturbances in the system increases, which conflicts with the control objective. Moreover, in its basic form, the auxiliary noise method converges slowly, and the modifications that

eliminate this problem are known to increase the complexity and computational cost of the controller considerably [25].

The most important commercial application of ANC systems are active headsets. Due to their small size, such systems typically employ feedback, and the high-frequency noise is canceled passively [18, 19, 28]. Closely related to active headsets are the active noise control motorcycle helmets [7, 30, 63, 74], which were demonstrated to offer a considerable reduction of noise. Another interesting application is ANC anti-snore system, which is very challenging due to severely limited freedom of placing the system's components and the variability of the secondary path, caused by movements of the sleeping person's head [8, 9, 26].

A highly promising area for ANC systems is the cancellation of acoustic noise generated by medical apparatus . The systems belonging to this category might aim at improving a patient's comfort or at reducing the long-term impact of the noise to medical staff. In the first group, one may point to an infant incubator ANC systems, where the purpose of the ANC system is to improve the infant's sleep quality and to eliminate the risk of hearing damage or loss [27, 31, 77]. In the second group, the active noise control of MRI noise stands out as the most important application [10, 11, 24, 62, 70].

Several other examples of interesting applications of ANC systems can be found in the survey paper [23].

2 Problem formulation

To simplify mathematical analysis, we will assume that all signals considered below, such as control signal, reference signal, narrowband disturbance and measurement noise are complex-valued. In section 5.2 we will describe a simple approach which allows one to use the obtained results when all signals are real-valued (which is a typical situation in practice.

Consider the problem of the reduction of a narrowband disturbance observed at the output of a discrete-time system (in acoustic applications this role is played by the secondary path) governed by the equation

$$y(t) = K_p(q^{-1})u(t-1) + d(t) + v(t) \tag{1}$$

where $t \in \mathbb{Z} = \{\ldots,-1,0,1,\ldots\}$ denotes normalized discrete time, $y(t)$ denotes the corrupted complex-valued output signal, q^{-1} is the backward shift operator, the signal

$$d(t) = a(t)e^{j\phi(t)}, \quad \phi(t) = \sum_{i=1}^{t} \omega(i) \tag{2}$$

is a complex-valued sinusoidal disturbance (cisoid) with a slowly-varying amplitude $a(t)$ and slowly-varying angular frequency $\omega(t) \in (-\pi,\pi]$, $v(t)$ denotes complex-valued wideband noise obeying the assumption

(A1) $\{v(t)\}$ is a sequence of independent complex-valued random variables with zero mean and variance σ_v^2; real and imaginary components of $v(t)$ are mutually independent,

and finally, $K_p(q^{-1})$ denotes transfer function of a stable, linear, single-input single output system obeying the condition

(A2) $K_p(e^{-j\omega}) \neq 0, \quad \forall \omega \in (-\pi, \pi]$.

Our goal will be to design a minimum-variance controller, i.e., to find such control rule which minimizes the signal observed at the output of the ANC system in the mean squared sense

$$u(t): \quad \mathrm{E}\left[|y(t)|^2\right] \longrightarrow \min \quad .$$

We will consider both purely feedback control strategies and hybrid strategies which combine feedback control and feedforward control (provided that the reference signal is available).

3 Feedback control strategies

3.1 Control in the case of full prior knowledge of the system and disturbance

Suppose that the transfer function of the system $K_p(q^{-1})$ is known and that disturbance has the form $d(t) = a_0 e^{j\omega_0 t}$ [which is equivalent to assuming that $a(t) \equiv a_0$ and $\omega(t) \equiv \omega_0$] and is measurable. To compensate sinusoidal disturbance of this form, one should generate such sinusoidal control signal $u(t)$ for which the system output, also sinusoidal due to system linearity, would have the same amplitude as $d(t)$ but opposite polarity. Since linear systems basically scale and shift sinusoidal inputs, the narrowband character of $u(t)$ justifies the following steady state approximation

$$K_p(q^{-1})u(t-1) = k_p u(t-1) \tag{3}$$

where $k_p = K_p(e^{-j\omega_0}) \in \mathbb{C}$ denotes the complex-valued system gain/attenuation at the frequency ω_0. Combining relationships (3) and (1), one obtains a simple formula $y(t) = k_p u(t-1) + d(t) + v(t)$, leading to the following form of control signal

$$u(t) = -\frac{d(t+1)}{k_p} \tag{4}$$

The steady state signal observed at the output of the open-loop system governed by (4) has the form $y(t) = v(t)$, which means that its variance takes the smallest achievable value equal to $\lim_{t\to\infty} \mathrm{E}[|y(t)|^2] = \sigma_v^2$.

3.2 Control in the case of full prior knowledge of the system and partial prior knowledge of the disturbance (known frequency)

Suppose that the amplitude of the disturbance with constant and known frequency ω_0 changes slowly with time according to the random walk model

$$a(t+1) = a(t) + \eta(t+1) \tag{5}$$

where the sequence of one-step amplitude changes $\{\eta(t)\}$ obeys the assumption

(A3) $\{\eta(t)\}$ is a sequence of independent random variables with zero mean and variance σ_η^2; the sequence $\{\eta(t)\}$ is independent of $\{v(t)\}$.

It is straightforward to check that under assumptions made above, the disturbance signal can be expressed in a recursive form

$$d(t+1) = e^{j\omega_0} d(t) + \widetilde{\eta}(t+1) \tag{6}$$

where $\{\widetilde{\eta}(t)\}$, $\widetilde{\eta}(t) = e^{j\omega_0}\eta(t)$, is a sequence of independent complex-valued random variables with zero mean and variance $\widetilde{\sigma}_\eta^2 = \sigma_\eta^2$.

Using the approximation $K_p(q^{-1})u(t-1) \cong k_p u(t-1)$, one can show that the optimal, minimum-variance control rule has the following steady state form [47]

$$\begin{aligned} \widehat{d}(t+1|t) &= e^{j\omega_0}[\widehat{d}(t|t-1) + \mu_a y(t)] \\ u(t) &= -\frac{\widehat{d}(t+1|t)}{k_p} \end{aligned} \tag{7}$$

where $\widehat{d}(t+1|t)$ denotes the predicted value of the disturbance and $\mu_a \in \mathbb{R}$ denotes the adaptation gain given by $\mu_a = -\xi/2 + \sqrt{\xi^2/4 + \xi}$, $\xi = \sigma_\eta^2/\sigma_v^2$. Under control rule (7), system output is given by $y(t) \cong c(t) + v(t)$, where

$$c(t) = d(t) - \widehat{d}(t|t-1) = e^{j\omega_0}(1-\mu_a)c(t-1) + \widetilde{\eta}(t) - \mu_a e^{j\omega_0} v(t+1) \tag{8}$$

is the quantity which will be further referred to as cancellation error. Based on this relationship it is easy to show that the steady state variance of the output signal is given by $\lim_{t\to\infty} \mathrm{var}[y(t)] = \sigma_c^2 + \sigma_v^2$, where $\sigma_c^2 = \lim_{t\to\infty} \mathrm{var}[c(t)] = \left[\sigma_\eta^2 + \sqrt{\sigma_\eta^4 + 4\sigma_\eta^2\sigma_v^2}\right]/2$.

3.3 Control in the case of partial prior knowledge of the system and partial prior knowledge of the disturbance (known frequency)

In practical situations the quantities k_p and μ_a not only are unknown but can also change over time due to the nonstationarity of the system and/or disturbance. Prior to designing an adaptive version of the controller, capable of automatic tuning of its settings, we will analyze properties of the "realistic" version of the controller (7)

$$\begin{aligned} \widehat{d}(t+1|t) &= e^{j\omega_0}[\widehat{d}(t|t-1)+\mu y(t)] \\ u(t) &= -\frac{\widehat{d}(t+1|t)}{k_n} \end{aligned} \tag{9}$$

obtained when the true system gain k_p is replaced with its "nominal" gain $k_n \neq k_p$, and when the optimal adaptation gain μ_a is replaced with an arbitrarily chosen gain $\mu \neq \mu_a$.

Denote by $\beta \in \mathbb{C}$, $\beta = k_p/k_n \neq 1$ the system gain modeling error. Similarly as in the optimal regulator case (7), the output signal can be expressed in the form $y(t) = c(t) + v(t)$ where now

$$c(t) = d(t) - \beta\widehat{d}(t|t-1) = e^{j\omega_0}(1-\mu\beta)c(t-1) + \widetilde{\eta}(t) - \mu\beta e^{j\omega_0}v(t+1) \tag{10}$$

Comparison of (8) and (10) leads to an interesting conclusion – when the adaptation gain coefficient μ is chosen so as to fulfill the condition

$$\mu\beta = \mu_a \tag{11}$$

the cancellation error (10) becomes identical with that yielded by the optimal controller (7). This means that by choosing the value of μ appropriately one can "compensate" the modeling error which is the consequence of adopting the inappropriate value of the system gain $k_n \neq k_p$. It is worth noticing that when $\mathrm{Im}[\beta] \neq 0$, the compensation mentioned above is possible provided that the adopted adaptation gain is complex-valued $\mu \in \mathbb{C}$. Having this in mind, we will design an adaptive algorithm for on-line tuning of a complex-valued adaptation gain μ. We will adjust μ recursively by minimizing the following local measure of fit, made up of exponentially weighted squares of system outputs

$$V(t;\mu) = \sum_{\tau=1}^{t} \rho^{t-\tau}|y(\tau;\mu)|^2 \tag{12}$$

where $\rho \in [0.999, 0.9999]$ denotes the so-called forgetting constant, determining the effective width of the local analysis window [in steady state equal to $1/(1-\rho)$ sampling intervals].

Using the method of recursive prediction error (RPE) [69], the following adaptive control algorithm, further referred to as SONIC (Self-Optimizing Narrowband Interference Canceller), was derived in [47] - see fig. 2

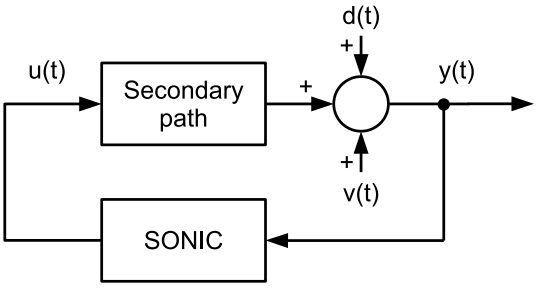

Fig. 2 Block diagram of an ANC system incorporating SONIC controller

$$
\begin{aligned}
z(t) &= e^{j\omega_0}\left[(1-c_\mu)z(t-1) - \frac{c_\mu}{\widehat{\mu}(t-1)}\,y(t-1)\right] \\
r(t) &= \rho r(t-1) + |z(t)|^2 \\
\widehat{\mu}(t) &= \widehat{\mu}(t-1) - \frac{z^*(t)y(t)}{r(t)} \\
\widehat{d}(t+1|t) &= e^{j\omega_0}[\,\widehat{d}(t|t-1) + \widehat{\mu}(t)y(t)\,] \\
u(t) &= -\frac{\widehat{d}(t+1|t)}{k_{\mathrm{n}}}
\end{aligned}
\tag{13}
$$

where $c_\mu \in [0.005, 0.05]$ denotes a small positive constant, and $z^*(t)$ denotes a complex conjugate of $z(t)$. The variable $z(t)$ is given by the formula

$$z(t) = \frac{\partial y(t;\mu)}{\partial \mu}$$

where

$$\frac{\partial}{\partial \mu} = \frac{1}{2}\left[\frac{\partial}{\partial \mathrm{Re}[\mu]} - j\,\frac{\partial}{\partial \mathrm{Im}[\mu]}\right]$$

denotes the so-called Wirtinger derivative [76], [6], [5], [21] – symbolic differentiation with respect to a complex variable [Wirtinger calculus facilitate minimization of nonanalytic functions of complex variables, such as (12)].

Without explaining details of the derivation, we will remark that it is based on the coefficient fixing technique, used to "robustify" self-tuning minimum-variance regulators [1]. Within this framework the value of one of system parameters is fixed and not estimated. It can be shown that this modeling error (the fixed value usually differs from the true value) is "corrected" when identification is carried out in the closed loop – in spite of the modeling bias the self-tuning regulator converges to the optimal regulator [41].

The self-optimization loop, made up of the first three recursions of SONIC, allows not only for compensation of the system modeling error ($\beta \neq 1$), but also for optimization of the controller. As shown in [47], under assumptions (A1)-(A3) it

holds that

$$\lim_{t\to\infty} \mathrm{E}[\widehat{\mu}(t)] \cong \frac{\mu_a}{\beta} \tag{14}$$

which means that the SONIC controller converges, in the mean sense, to the optimal controller (7). Even more importantly, since optimization of μ is performed using the RPE approach, the controller (13) will attempt to minimize the cancellation error also in cases where the assumptions (A1)-(A3) – not very realistic from the practical viewpoint – are not fulfilled, i.e., it should respond adequately to the changes in plant dynamics, changes of the signal-to-noise ratio ξ, etc.

The robustness of SONIC can be demonstrated using a simple simulation experiment, carried out for a system with switched dynamics – all details are given in table 1. The narrowband disturbance and wideband noise were generated using the following settings: $\sigma_v = 0.1$, $\sigma_e = 0.001$, $\omega_0 = 0.1$, $d(0) = 1$.

Time interval	System	$\lvert\beta\rvert$	Argβ[°]
$0 < t < 15000$	$K_1(z) = \dfrac{0.0952}{1-0.9048z^{-1}}$	0.708	-47.9
$15000 \le t < 30000$	$K_2(z) = \dfrac{0.0238}{1-0.9762z^{-1}}$	0.234	-79.3
$30000 \le t < 45000$	$K_3(z) = \dfrac{0.2}{1-0.8z^{-1}}$	0.913	-27.1
$45000 \le t \le 60000$	$K_4(z) = \dfrac{+0.1-0.14z^{-1}}{1-1.8391z^{-1}+0.8649z^{-2}}$	1.960	121.1

Table 1 System switching schedule in the transient behavior experiment and the corresponding modeling errors.

While the first two changes [from $K_1(q^{-1})$ to $K_2(q^{-1})$ at instant $t = 15000$ and from $K_2(q^{-1})$ to $K_3(q^{-1})$ at instant $t = 30000$] were confined to plant parameters, the last change was more substantial: at instant $t = 45000$, the first-order inertial system $K_3(q^{-1})$ with a single real pole was switched to the second-order nonminimum phase system $K_4(q^{-1})$ with a pair of complex poles. Since the phase shift introduced by $K_4(q^{-1})$ at the frequency ω_0 differs from the analogous shift of $K_3(q^{-1})$ by more than $\pi/2$, the last change causes temporal instability of the closed-loop system, making the task of disturbance rejection even harder.

Fig. 3 (illustrating typical behavior) and Fig. 4 (illustrating mean behavior) show results obtained for the SONIC algorihm with the following settings: $c_\mu = 0.005$, $\rho = 0.9995$, $k_n = e^{j\omega_0}$. Additionally, the algorithm was equipped with sefety jacketing mechanisms which will be described in section 5.1 [with $\mu_{\max} = 0.05$, $\mu_{\min} = 0$, $\Delta\mu_{\max}(t) = \widehat{\mu}(t-1)/50$, $r_{\max} = 1600$, $r_{\min} = 0$].

The adaptation process was started at instant $t = 1$ using the following initial conditions: $\widehat{d}(0) = e^{j\omega_0}$, $r(0) = 100$, $z(0) = 0$, $\widehat{\mu}(0) = 0.02$. The algorithm copes favorably with both the initial convergence problem and with abrupt plant changes. When the experiment is started or when a change to the plant dynamics occurs, the magnitude of the adaptation gain $\widehat{\mu}(t)$ temporarily increases to quickly compensate large initial modeling errors; later on, it gradually decays to settle down around its optimal steady state value. Note the very quick response to phase errors and usually much slower response to magnitude errors — the effect caused by diverse sensitivity of system output to two types of modeling errors.

The simulation experiment shows also that the proposed control scheme has a self-stabilization property. When instability occurs at the instant $t = 45000$ [which is unavoidable since, due to the sign mismatch, the stabilizing gain $\widehat{\mu}$ for $K_3(q^{-1})$ does not stabilize $K_4(q^{-1})$], it causes rapid growth of the output signal $y(t)$, which in turn speeds up convergence of $\widehat{\mu}$ to a new stabilizing value. In this way, after a burst observed at the system output, the closed-loop stability is regained.

3.4 Control in the case of partial prior knowledge of the system and partial prior knowledge of the disturbance (unknown frequency)

Suppose that the frequency $\omega(t)$ of the narrowband disturbance is not known and slowly varies with time. Prior to designing the fully adaptive minimum-variance regulator, we will analyze properties of the modified algorithm (9), obtained by means of replacing the known frequency ω_0 with the current estimate of the instantaneous frequency

$$\begin{aligned} \widehat{d}(t+1|t) &= e^{j\widehat{\omega}(t|t-1)}[\widehat{d}(t|t-1) + \mu y(t)] \\ \widehat{\omega}(t+1|t) &= g[\mathscr{Y}(t)] \\ u(t) &= -\frac{\widehat{d}(t+1|t)}{k_n} \end{aligned} \tag{15}$$

where $\widehat{\omega}(t+1|t)$ denotes the one-step-ahead prediction of the instantaneous frequency $\omega(t+1)$ based on observations $\mathscr{Y}(t) = \{y(i), i \le t\}$ gathered up to the instant t.

Estimation of the instantaneous frequency can be carried out using a simple gradient algorithm [48]

$$\widehat{\omega}(t+1|t) = \widehat{\omega}(t|t-1) + \gamma \mathrm{Arg}\left[\frac{\widehat{d}(t+1|t)e^{-j\widehat{\omega}(t|t-1)}}{\widehat{d}(t|t-1)}\right] \tag{16}$$

where γ, $0 < \gamma \ll 1$ denotes adaptation gain in the frequency estimation loop, and $\mathrm{Arg}(\cdot) \in (-\pi, \pi]$ denotes the principal argument of a complex number. In the case of

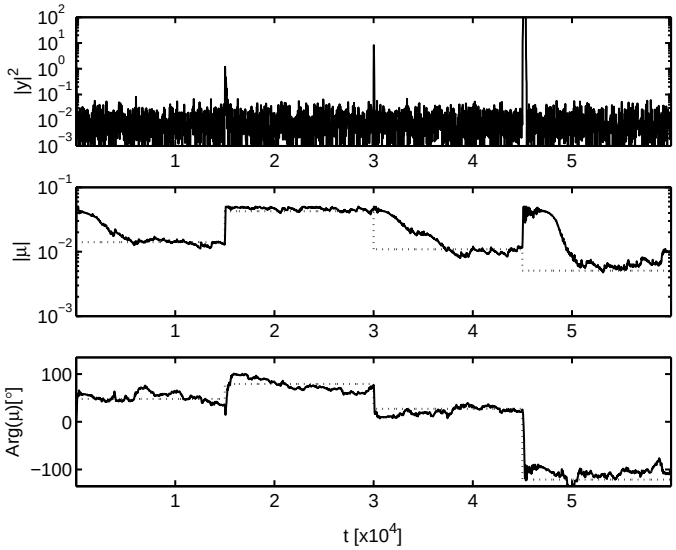

Fig. 3 Typical simulation results obtained using SONIC. Solid lines – the estimated quantities, dotted lines – optimal steady state values.

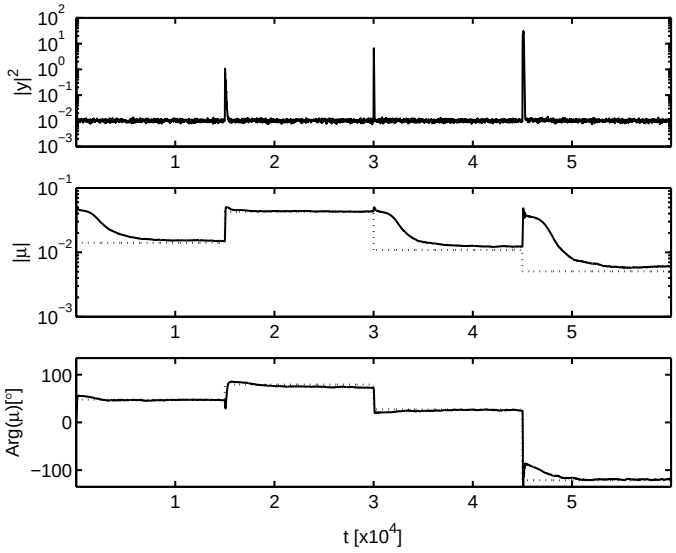

Fig. 4 Simulation results obtained using SONIC, averaged over 100 process realizations. Solid lines – the estimated quantities, dotted lines – optimal steady state values.

slowly time-varying disturbance signals, one can use the following approximation

$$\mathrm{Arg}\left[\frac{\widehat{d}(t+1|t)e^{-j\widehat{\omega}(t|t-1)}}{\widehat{d}(t|t-1)}\right]=\mathrm{Im}\left\{\log\left[1+\frac{\mu y(t)}{\widehat{d}(t|t-1)}\right]\right\}\cong\mathrm{Im}\left[\frac{\mu y(t)}{\widehat{d}(t|t-1)}\right]$$

which leads to the following control algorithm

$$\begin{aligned}\widehat{d}(t+1|t)&=e^{j\widehat{\omega}(t|t-1)}[\widehat{d}(t|t-1)+\mu y(t)]\\ \widehat{\omega}(t+1|t)&=\widehat{\omega}(t|t-1)+\gamma\mathrm{Im}\left[\frac{\mu y(t)}{\widehat{d}(t|t-1)}\right]\\ u(t)&=-\frac{\widehat{d}(t+1|t)}{k_n}\end{aligned}\tag{17}$$

Analysis of tracking properties of the algorithm (17) can be performed using the method of local averaging [2] and the approximating linear filtering (ALF) technique [44, 71], developed for the purpose of studying adaptive notch filters (ANF). Consider a local analysis window $T=[t_1,t_2]$ of width $n=t_2-t_1+1$ obeying the condition $n\gg 2\pi/\omega(t)$, $\forall t\in T$. Assuming that $K_p(e^{-j\omega})$ is a smooth function of ω, that the amplitude of the disturbance is constant and equal to a_0, and that the instantaneous frequency $\omega(t)$ varies slowly with time, the output of a system excited by a narrowband input signal can be approximately expressed in the form $K_p(q^{-1})u(t-1)\cong k_T u(t-1)$, $t\in T$, where $k_T=\sum_{t\in T}K_{\mathrm{p}}(e^{-j\omega(t)})/n$ denotes the mean gain of the system in the time interval T. Using this approximation, the output signal can be expressed in the form $y(t)\cong d(t)-\beta\widehat{d}(t|t-1)+v(t),t\in T$, where $\beta=k_T/k_n$. Denote by $w(t)$ the one-step change of the instantaneous frequency

$$\omega(t)=\omega(t-1)+w(t).$$

The ALF technique amounts to studying dependence between the cancellation error $c(t)=d(t)-\beta\widehat{d}(t|t-1)$ and frequency tracking error $\Delta\widehat{\omega}(t)=\omega(t)-\widehat{\omega}(t|t-1)$, and "exciting" signals $v(t)$ i $w(t)$, while neglecting all moments of these quantities of order higher than 1, as well as all "cross-terms". Using this approach, one arrives at the following linear relationships

$$\begin{aligned}\Delta\widehat{x}(t)&=(1-\mu\beta)\Delta\widehat{x}(t-1)+ja_0^2\Delta\widehat{\omega}(t-1)\mu\beta s(t-1)\\ \Delta\widehat{\omega}(t+1)&=\Delta\widehat{\omega}(t)-\frac{\gamma}{a_0^2}\mathrm{Im}[\mu\beta\Delta\widehat{x}(t)]-\frac{\gamma}{a_0^2}\mathrm{Im}[\mu\beta z(t)]+w(t+1)\end{aligned}\tag{18}$$

where $\Delta x(t)=c(t)d^*(t)$ and $s(t)=v(t)d^*(t)$.

Equations of the linear approximating filter (18) allow one to quantify frequency tracking errors. Note that – similar to (10) – both ALF equations incorporate terms that depend on $\mu\beta$, and neither of them incorporates terms dependent exclusively on μ or β. This means that, also in this case, system modeling errors can be compensated by a suitable choice of a complex-valued gain μ.

Interesting analytical results can be obtained in the case where the instantaneous frequency evolves according to the random walk model, i.e., when

(A4) $\{w(t)\}$ is a sequence of zero-mean independent random variables with variance σ_w^2; the sequence $\{w(t)\}$ is independent of $\{v(t)\}$ and $\{\eta(t)\}$.

Assume, for simplicity, that the true system gain is known ($\beta = 1$), which means that there is no need to adopt complex-valued gain μ, i.e., $\mu \in \mathbb{R}$. Let $s_I(t) = \mathrm{Im}[s(t)]$. Under the restrictions mentioned above the following result can be obtained after solving ALF equations

$$\Delta\widehat{\omega}(t) \cong H_1(q^{-1})s_I(t) + H_2(q^{-1})w(t)$$

where

$$H_1(q^{-1}) = -\frac{\eta\mu(1-q^{-1})q^{-1}}{a^2[1-(1+\lambda)q^{-1}+(\lambda+\eta\mu)q^{-2}]}$$

$$H_2(q^{-1}) = \frac{1-\lambda q^{-1}}{1-(1+\lambda)q^{-1}+(\lambda+\eta\mu)q^{-2}}$$

and $\lambda = 1-\mu$. Linear filters $H_1(q^{-1})$ and $H_2(q^{-1})$ are asymptotically stable for all values $\mu, \gamma \in (0,1)$. Since under the assumption (A4) the processes $\{s_I(t)\}$ and $\{w(t)\}$ are orthogonal, the steady state expression for the variance of the frequency tracking error takes the form

$$\mathrm{E}\{[\Delta\widehat{\omega}(t)]^2\} = I[H_1(z^{-1})]\mathrm{E}[s_\mathrm{I}^2(t)] + I[H_2(z^{-1})]\mathrm{E}[w^2(t)]$$

where

$$I[X(z^{-1})] = \frac{1}{2\pi j}\oint X(z)X(z^{-1})\frac{dz}{z}$$

is an integral evaluated along the unit circle in the $\mathscr{Z}$-plane, and $X(z^{-1})$ denotes any stable proper rational transfer function. Using the method of residue calculus [22] and taking into account the facts that $\mathrm{E}[s_\mathrm{I}^2(t)] = a_0^2\sigma_v^2/2$ and $\mathrm{E}[w^2(t)] = \sigma_v^2$, one arrives at

$$\mathrm{E}[(\Delta\widehat{\omega}(t))^2] \cong \frac{\gamma^2\mu}{4a_0^2}\,\sigma_v^2 + \left[\frac{1}{2\gamma} + \frac{1}{2\mu}\right]\sigma_w^2\,. \tag{19}$$

Denote by μ_ω and γ_ω the coefficints that minimize the mean squared error (19). Straightforward calculations lead to

$$\mu_\omega = \sqrt[4]{8\zeta}, \quad \gamma_\omega = \sqrt[4]{\zeta/2}, \quad \zeta = \frac{a_0^2\sigma_w^2}{\sigma_v^2}$$

and

$$\mathrm{E}[(\Delta\widehat{\omega}(t))^2\,|\,\mu_\omega,\gamma_\omega] \cong \sigma_w^2\sqrt[4]{2\zeta^{-1}}\,. \tag{20}$$

The mean squared frequency estimation error cannot be smaller than the so-called *a posteriori* Craméra-Rao lower (PCRB)[1] As shown in [71], when the variables $v(t)$ and $w(t)$ are normally distributed, PCRB takes the form

$$\mathrm{PCRB} \cong \sigma_w^2 \sqrt[4]{2\zeta^{-1}} \,. \tag{21}$$

Comparison of relationships (20) and (21) leads to the conclusion that the optimally tuned algorithm (17) is – in spite of its very simple form – statistically efficient, i.e., it guarantees the highest achievable estimation accuracy when the instantaneous frequency $\omega(t)$ drifts in a random way. More than that, as shown in the paper [54], under more realistic frequency variation scenarios the simple gradient algorithm (17) yields results that are comparable with those obtained by means of applying the high-resolution (and computationally much more demanding) frequency estimation algorithm known as ESPRIT (Estimation of Signal Parameters via Rotational Invariance Techniques) [32].

Combining all adaptation mechanisms described so far, one obtains the following extended version of the SONIC algorithm [48]

$$\begin{aligned}
&self-optimization \\
z(t) &= e^{j\widehat{\omega}(t|t-1)} \left[(1-c_\mu) z(t-1) - \frac{c_\mu}{\widehat{\mu}(t-1)} y(t-1) \right] \\
p(t) &= \rho r(t-1) + |z(t)|^2 \\
\widehat{\mu}(t) &= \widehat{\mu}(t-1) - \frac{y(t) z^*(t)}{p(t)}
\end{aligned} \tag{22}$$

$$\begin{aligned}
&predictive\ control \\
\widehat{d}(t+1|t) &= e^{j\widehat{\omega}(t|t-1)} [\widehat{d}(t|t-1) + \widehat{\mu}(t) y(t)] \\
u(t) &= -\frac{\widehat{d}(t+1|t)}{k_{\mathrm{n}}[\widehat{\omega}(t|t-1)]}
\end{aligned} \tag{23}$$

$$frequency\ estimation$$

$$\widehat{\omega}(t+1|t) = \widehat{\omega}(t|t-1) + \gamma \mathrm{Im} \left[\frac{\widehat{\mu}(t) y(t)}{\widehat{d}(t|t-1)} \right] \tag{24}$$

where c_μ, ρ, γ and $k_n[\widehat{\omega}(t|t-1)] = K_n(e^{j\widehat{\omega}(t|t-1)})$ are previously defined regulator settings, and $K_n(q^{-1})$ denotes the "nominal" transfer function of the system. If no prior knowledge about the system is available, one can set $K_n(q^{-1}) \equiv 1$.

[1] Since in the case considerd $\omega(t)$ is a random variable (rather than an unknown deterministic constant) the classical Craméra-Rao bound does not apply.

Fig. 5 shows typical results obtained for a real-valued system. The algorithm (22)-(24), after modifications described in sections 5.1-5.2, was implemented on a regular PC. The sampling rate was equal to 1 kHz. The left loudspeaker was used to generate disturbance, and the right one – to generate the antisound. The error microphone was placed 15 cm away from the right loudspeaker. The instantaneous frequency of the disturbance was slowly varying, in a sinusoidal way, between 241 Hz and 250 Hz with a period equal to 20 seconds. The nominal gain of the system was set to $k_n = 1$ and the remaining settings of SONIC were equal to: $c_\mu = 0.01$, $\mu_{\max} = 0.05$, $\gamma = 0.01$. Application of the extended SONIC led to attenuation of the harmonic noise which, depending on the instantaneous frequency, ranged between 15 and 20 dB.

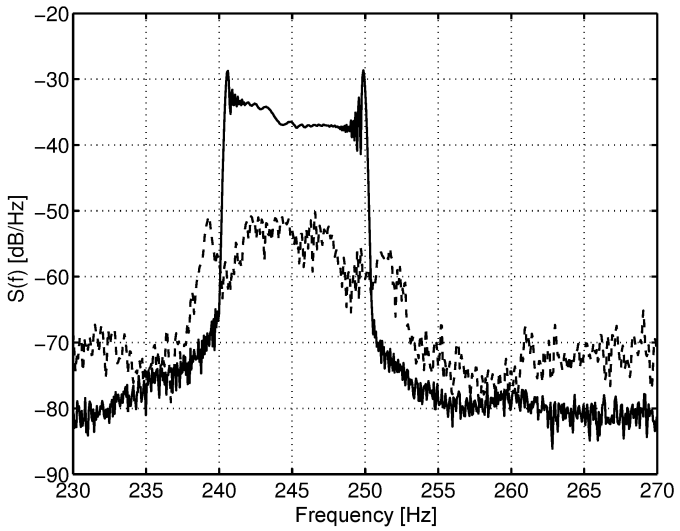

Fig. 5 Comparison of spectral density functions of disturbances observed at the output of a real acoustic system: without control (solid line) and under control of the extended SONIC algorithm (broken line).

4 Control incorporating both feedback and feedforward mechanisms

An obvious advantage of SONIC, typical of all feedback ANC systems, is due to the fact that it does not require deployment of a reference sensor. Such a sensor may be expensive and/or difficult to mount. Additionally, it may introduce acoustic feedback, which deteriorates performance of the ANC system. However, this advantage comes at a price: without access to a reference signal, SONIC needs to learn the

properties of the disturbance, such as its instantaneous frequency $\omega(t)$, by observing the error signal $y(t)$, i.e., the very signal it is trying to cancel. Such an internal "conflict of interests" (things that are good for identification are bad for control and *vice versa*) is an inherent limitation of many adaptive control systems. Under nonstationary conditions, this may result in episodes of turbulent, or even bursting, behavior, not acceptable from a practical viewpoint. Additionally, fluctuations of the attenuation rate (since periods of higher attenuation are interleaved with periods of lower attenuation), even if in a small range, make the residual noise less comfortable for a human listener than a constant-intensity noise.

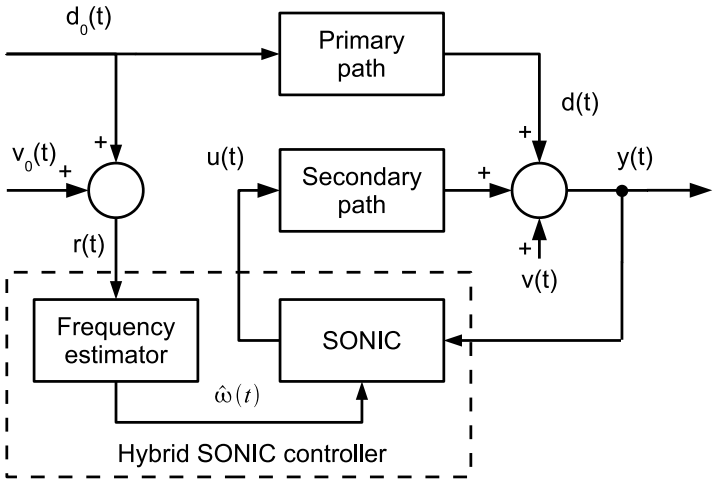

Fig. 6 Block diagram of the ANC system incorporating hybrid SONIC controller.

The drawbacks described above can be eliminated by equipping the control system with a reference sensor (microphone, accelerator), placed close to the source of the unwanted sound, and measuring the reference signal

$$r(t) = d_*(t) + v_*(t) \tag{25}$$

where $d_*(t)$ denotes the reference disturbance, strongly correlated with $d(t)$, and $v_*(t)$ denotes sensor noise, independent of $v(t)$. The proposed solution is obtained by replacing in SONIC the estimate $\widehat{\omega}(t|t-1)$ yielded by the feedback frequency estimation loop, with a suitably modified (smoothed or simply delayed) estimate of the instantaneous frequency $\omega_*(t)$ of the signal $d_*(t)$, obtained by means of processing the reference signal $r(t)$. Such a hybrid feedforward/feedback solution, depicted in Fig. 6, has several advantages over a purely feedback design. First, the reference signal is a non-vanishing source of information about the instantaneous frequency of the disturbance. Secondly, even if the ANC system is switched off, the signal-to-noise ratio is usually much higher at the reference point than at the cancellation

point. Finally, since the reference signal is measured ahead of time, estimation of the instantaneous frequency of $d(t)$ can be based not only on the past, but also on a certain number of "future" (relative to the local time of the controller) samples of the disturbance. Such noncausal estimates, which incorporate smoothing, are more accurate than their causal counterparts.

The instantaneous frequency $\omega_*(t)$ of the signal $d_*(t)$ can be estimated using a slightly modified version of the algorithm used to track the signal $d(t)$

$$\begin{aligned} \varepsilon(t) &= r(t) - \widehat{d}_*(t|t-1) \\ \widehat{d}_*(t+1|t) &= e^{j\widehat{\omega}_*(t)}[\widehat{d}_*(t|t-1) + \mu_*\varepsilon(t)] \\ \widehat{\omega}_*(t+1) &= \widehat{\omega}_*(t) + \gamma_*\mu_* \operatorname{Im}\left[\frac{\varepsilon(t)}{\widehat{d}_*(t|t-1)}\right] \end{aligned} \tag{26}$$

where μ_* and γ_*, $0 < \mu_*, \gamma_* \ll 1$, denote small adaptation gains. Unlike the coefficient μ in the algorithm (24), the coefficient μ_* in (26) is constant and real-valued.

Using the ALF approach, one can show that if the frequency $\omega_*(t)$ changes slowly, the quantity $\widehat{\omega}_*(t)$ can be viewed as an approximately unbiased estimate of $\omega_*(t-\tau_{\text{est}})$, where $\tau_{\text{est}} = \text{int}[t_\omega]$, $t_\omega = 1/\gamma_*$, denotes the so-called estimation delay [42] introduced by the algorithm (26). This is a straightforward consequence of the fact that the mean trajectory of the estimates $\widehat{\omega}_*(t)$ is delayed with respect to the true trajectory $\omega_*(t)$ by (approximately) τ_{est} sampling intervals [59]. Due to the causality principle, in a majority of adaptive control applications estimation of unknown system/signal coefficients can be based exclusively on past data samples. In the case of the ANC system depicted in Fig. 6 the situation is different. Since the acoustic delay, i.e., delay with which the sound wave emitted by the source of disturbance reaches the point at which it is supposed to be canceled, is considerably longer than the electrical delay with which reference measurements are transmitted to the control unit, the controller has the advantage of knowing the disturbance (or, more precisely, of knowing the signal correlated with the disturbance) before it reaches the cancellation point. Denote by τ_{el} the electrical delay, by $\tau_{\text{ak}} \gg \tau_{\text{el}}$ – the acoustic delay, and by τ_{prz} – the time needed to complete one cycle of computations using the algorithm (26). Since it holds approximately that $\omega(t) \cong \omega_*(t-\tau_{\text{ak}})$, when the processing unit is sufficiently fast the control algorithm has at its disposal the estimate of the instantaneous frequency of $d(t)$ with a time advance equal to $\tau_0 = \tau_{\text{ak}} - \tau_{\text{el}} - \tau_{\text{prz}}$ sampling intervals. Hence, after accounting for the estimation delay, as an estimate of the instantaneous frequency $\omega(t)$, one can use the following quantity

$$\widehat{\omega}(t) = \widehat{\omega}_*(t-\tau_{\text{d}}) \tag{27}$$

where $\tau_{\text{d}} = \max\{\tau_0 - \tau_{\text{est}}, 0\}$. When $\tau_0 < \tau_{\text{est}}$ only a partial correction of the bias can be achieved.

The hybrid SONIC algorithm incorporating both feedback and feedforward mechanisms has the form

$$
\begin{aligned}
z(t) &= e^{j\widehat{\omega}_*(t-\tau_{\mathrm{d}})}\left[(1-c_\mu)z(t-1)-\frac{c_\mu}{\widehat{\mu}(t-1)}y(t-1)\right]\\
p(t) &= \rho r(t-1)+|z(t)|^2\\
\widehat{\mu}(t) &= \widehat{\mu}(t-1)-\frac{y(t)z^*(t)}{p(t)}\\
\widehat{d}(t+1|t) &= e^{j\widehat{\omega}_*(t-\tau_{\mathrm{d}})}[\widehat{d}(t|t-1)+\widehat{\mu}(t)y(t)]\\
u(t) &= -\frac{\widehat{d}(t+1|t)}{k_{\mathrm{n}}[\widehat{\omega}_*(t-\tau_{\mathrm{d}})]}
\end{aligned}
\tag{28}
$$

where $\widehat{\omega}_*(t)$ denotes the estimate of the instantaneous frequency of the reference signal $d_*(t)$ obtained using the algorithm (26).

Unlike most of the existing hybrid schemes, hybrid SONIC is not made up of two controllers – the reference signal is used only to extract information about the instantaneous frequency of the disturbance, rather than to form the reference-dependent control (compensation) signal. Therefore it can be characterized as a feedback ANC with an external (feedforward) frequency adjustment mechanism. Since the reference signal is usually a more reliable source of information about the instantaneous frequency of the disturbance than the error signal (which is minimized by the controller), hybrid SONIC has better tracking and robustness properties than its original, purely feedback version.

Time shift is the simplest form of noncausal estimation of the frequency $\omega_*(t)$ [45]. The estimation accuracy can be further improved by means of application of the fixed-delay adaptive notch smoothing (ANS) algorithm

$$\widehat{\omega}(t)=\widehat{\omega}_*(t-\tau_{\mathrm{d}}|t) \tag{29}$$

where $\widehat{\omega}_*(t-\tau_{\mathrm{d}}|t)$ denotes the estimate of the frequency at the instant $t-\tau_{\mathrm{d}}$ based on the data collected up to the instant t, i.e., data incorporating τ_{d} "future" measurements of the reference signal. The ANS algorithms of this form were presented in [43, 46, 52, 55].

The properties of the hybrid SONIC algorithm were checked in a simulation experiment incorporating a realistic model of the controlled system obtained via identification. The aim of this experiment was to compare the algorithms (22)-(24) and (28). The simulated sampling rate was equal to 8kHz. The assumed transportation delays introduced by the primary path and secondary path were equal to 100 and 60 sampling intervals, respectively. The instantaneous frequency of the disturbance was varying between 190 Hz and 210 Hz. Finally, the nominal gain of the secondary path was set to its true gain measured at the frequency 200 Hz.

The results of the experiment are shown in Fig. 7. Note fluctuations of the amplitude of the residual output signal in the case which can be observed when the frequency of the disturbance is estimated in the feedback loop – the effect caused by periodic deterioration of identifiability conditions caused by operation of the control loop. Note also that no such effect appears when the hybrid algorithm is used, which results in the improvement of cancellation efficiency by 5-15 dB.

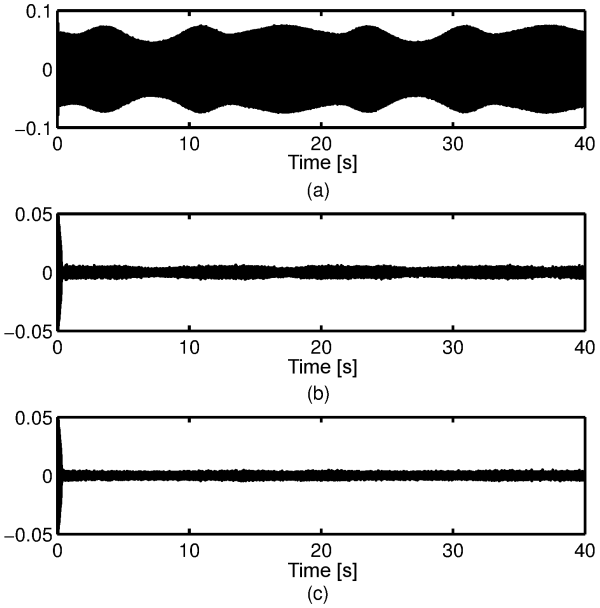

Fig. 7 Comparison of signals observed at the output of the simulated acoustic system. (a) Without active noise cancellation. (b) Obtained using the extended SONIC controller (c) Obtained using the hybrid SONIC controller.

5 Extensions

5.1 Recommended safety guards

To robustify the SONIC controller against abrupt changes of plant and/or disturbances (e.g. the changes of nonstationarity level of the disturbance, measurement noise variance, impulsive disturbances), and to improve its behavior during the initial transient phase, one may employ several heuristic modifications.

Excessive variability of the adapted parameters may be prevented by upper-bounding the magnitude of the complex gain $|\widehat{\mu}(t)|$, its one-step changes $|\widehat{\mu}(t) - \widehat{\mu}(t-1)|$, and the scaling variable $r(t)$. These modifications can be regarded as safety guards typical to adaptive control. Additionally, to prevent the shutdown of the algorithm, it is recommended to introduce additional lower bounds on the variables $\widehat{\mu}(t)$ and $r(t)$.

Denote by $\mathrm{clip}(x,a,b),\ x \in \mathrm{C},\ \mathrm{a,b} \in \mathrm{R}_+$ the complex clip function

$$\mathrm{clip}(x,a,b) = \begin{cases} a\frac{x}{|x|} & \text{dla} \quad |x| < a \\ x & \text{dla} \quad a \le |x| \le b \\ b\frac{x}{|x|} & \text{dla} \quad |x| > b \end{cases} .$$

The modified algorithm (13) has the form

$$\begin{aligned} z(t) &= e^{j\omega_0}\left[(1-c_\mu)z(t-1) - \frac{c_\mu}{\widehat{\mu}(t-1)}y(t-1)\right] \\ r(t) &= \mathrm{clip}(\rho r(t-1) + |z(t)|^2, r_{\min}, r_{\max}) \\ \Delta\widehat{\mu}(t) &= \mathrm{clip}(\frac{z^*(t)y(t)}{r(t)}, 0, \Delta\mu_{\max}) \\ \widehat{\mu}(t) &= \mathrm{clip}(\widehat{\mu}(t-1) - \Delta\widehat{\mu}(t), \mu_{\min}, \mu_{\max}) \\ \widehat{d}(t+1|t) &= e^{j\omega_0}[\widehat{d}(t|t-1) + \widehat{\mu}(t)y(t)] \\ u(t) &= -\frac{\widehat{d}(t+1|t)}{k_n}\,. \end{aligned} \tag{30}$$

5.2 Modifying the SONIC controller to work with real-valued signals and systems

A variant of the SONIC controller designed to work with real-valued signals was derived in [49]. It was assumed that the controlled plant is governed by eq. (1), and the assumptions regarding the disturbance signals were modified. The measurement noise $v(t)$ was modeled as real-valued Gaussian-distributed zero-mean white noise with variance σ_v^2, and the narrowband disturbance $d(t)$ as governed by

$$\begin{aligned} d(t) &= \boldsymbol{\alpha}^{\mathrm{T}}(t)\mathbf{f}(t) \\ \boldsymbol{\alpha}(t) = [\alpha_1(t), \alpha_2(t)]^{\mathrm{T}},\ \mathbf{f}(t) &= [\sin(\omega_0 t), \cos(\omega_0 t)]\,, \end{aligned} \tag{31}$$

where the vector $\boldsymbol{\alpha}(t)$ is a two-dimensional random walk process

$$\begin{aligned} \boldsymbol{\alpha}(t+1) &= \boldsymbol{\alpha}(t) + \mathbf{e}(t) \\ \mathbf{e}(t) = [e_1(t)\ e_2(t)],\ \mathbf{e}(t) &\sim \mathscr{N}(\mathbf{0}, \sigma_e^2\mathbf{I})\,, \end{aligned}$$

which can be regarded as a real-valued counterpart of the complex-valued disturbance governed by (2) and (5).

The inner control loop proposed in [49] takes the form

$$\begin{aligned} \widehat{\boldsymbol{\alpha}}(t+1|t) &= \widehat{\boldsymbol{\alpha}}(t|t-1) + \hat{\mathbf{M}}(t)\mathbf{f}(t)y(t) \\ u(t) &= -\widehat{\boldsymbol{\alpha}}^{\mathrm{T}}(t)\mathbf{K}_n\mathbf{f}(t)\,, \end{aligned} \tag{32}$$

where $\widehat{\alpha}(t+1|t)$ is the one-step prediction of the vector $\alpha(t)$,

$$\mathbf{K}_n = \begin{bmatrix} \mathrm{Re}[K_n(e^{j\omega_0})] & \mathrm{Im}[K_n(e^{j\omega_0})] \\ -\mathrm{Im}[K_n(e^{j\omega_0})] & \mathrm{Re}[K_n(e^{j\omega_0})] \end{bmatrix}$$

denotes the nominal gain matrix of the plant at frequency ω_0, and

$$\hat{\mathbf{M}}(t) = \begin{bmatrix} \mathrm{Re}[\widehat{\mu}(t)] & -\mathrm{Im}[\widehat{\mu}(t)] \\ \mathrm{Im}[\widehat{\mu}(t)] & \mathrm{Re}[\widehat{\mu}(t)] \end{bmatrix}$$

where $\widehat{\mu}(t)$ is the complex-valued gain coefficient, whose value is adjusted in the outer self-optimization loop.

The self-optimization loop reads

$$\begin{aligned} z_y(t) &= -c_\mu \mathbf{f}^{\mathrm{T}}(t)\hat{\mathbf{M}}^{-1}(t-1)\mathbf{z}_\alpha(t-1) \\ \mathbf{z}_\alpha(t) &= \mathbf{z}_\alpha(t-1) + \hat{\mathbf{M}}(t-1)\mathbf{f}(t)z_y(t) + \mathbf{H}\mathbf{f}(t)y(t) \\ r(t) &= \rho r(t) + |z_y(t)|^2 \\ \widehat{\mu}(t) &= \widehat{\mu}(t-1) - \frac{z_y^*(t)y(t)}{r(t)} \,, \end{aligned}$$

where $c_\mu > 0$ is a small constant and

$$\mathbf{H} = \frac{\partial \mathbf{M}}{\partial \mu} = \frac{1}{2}\begin{bmatrix} 1 & j \\ -j & 1 \end{bmatrix}, \quad \mathbf{M} = \begin{bmatrix} \mathrm{Re}[\mu] & -\mathrm{Im}[\mu] \\ \mathrm{Im}[\mu] & \mathrm{Re}[\mu] \end{bmatrix} \,,$$

The above equations were derived using the approach similar to the complex-valued case, i.e., using the Wirtinger calculus and the coefficient fixing technique.

Remarkably, one may obtain almost exactly the same control results using algorithm (13), modified by projecting the complex control signal on the real axis [34]

$$\begin{aligned} z(t) &= e^{j\omega_0}\left[(1-c_\mu)z(t-1) - \frac{c_\mu}{\widehat{\mu}(t-1)}y(t-1)\right] \\ r(t) &= \rho r(t-1) + |z(t)|^2 \\ \widehat{\mu}(t) &= \widehat{\mu}(t-1) - \frac{z^*(t)y(t)}{r(t)} \\ \widehat{d}(t+1|t) &= e^{j\omega_0}[\widehat{d}(t|t-1) + \widehat{\mu}(t)y(t)] \\ u(t) &= -\mathrm{Re}\left[\frac{\widehat{\mathrm{d}}(\mathrm{t}+1|\mathrm{t})}{\mathrm{k_n}}\right] \,. \end{aligned} \tag{33}$$

Taking into account the effort required to develop real-valued versions of algorithms (22)-(24), (26)-(28) from scratch, one is allowed to conclude that the projection method is the recommended approach to the implementation of the SONIC-family controllers in real-world systems.

5.3 Application of improved estimators of instantaneous frequency

In many applications, the instantaneous frequency of disturbances varies in, approximately, a piecewise linear way. In such cases, the estimates obtained using the algorithm (16) will be biased, which will affect the cancellation performance of the controller adversely. To mitigate this issue, an improved version of the frequency estimator, which equips it with the capability to track the local trend in the frequency trajectory, was proposed in [51]. The extended algorithm has the form

$$\begin{aligned}\widehat{\alpha}(t+1|t) &= \widehat{\alpha}(t|t-1) + \gamma_\alpha g(t)\\ \widehat{\omega}(t+1|t) &= \widehat{\omega}(t|t-1) + \widehat{\alpha}(t+1|t) + \gamma_\omega g(t)\\ g(t) &= \mathrm{Arg}\left[\frac{\widehat{d}(t+1|t)}{\widehat{d}(t|t-1)e^{j\widehat{\omega}(t|t-1)}}\right],\end{aligned} \tag{34}$$

where $\widehat{\alpha}(t+1|t)$ and $\widehat{\omega}(t+1|t)$ denote the one-step predictions of frequency rate and frequency, respectively, while γ_α and γ_ω are small gains that satisfy the condition $0 \leq \gamma_\alpha \ll \gamma_\omega$. Note that, for $\gamma_\alpha = 0$ and zero initial conditions, the algorithm (34) reduces to (16).

Behavior of the algorithm (34) was analyzed using the approximating linear filter approach, under the assumption that the instantaneous frequency is governed by the following model

$$\begin{aligned}\omega(t+1) &= \omega(t) + \alpha(t+1)\\ \alpha(t+1) &= \alpha(t) + w_\alpha(t+1),\end{aligned} \tag{35}$$

where $\omega(t)$ and $\alpha(t)$ denote the frequency and frequency rate, respectively, and $\{w_\alpha(t+1)\}$ is the sequence of one-step changes of the process $\alpha(t)$. The analysis demonstrated that the proposed improved estimator is statistically efficient. Moreover, simulation results presented in [51] demonstrate that the application of the extended frequency estimator can result in 5 to 15 dB of improvement in the cancellation performance of the SONIC controller.

5.4 Extension to the multifrequency case

The control algorithms presented so far are capably only of canceling sinusoidal disturbances. In many applications, however, one may encounter the need to cancel nonsinusoidal disturbances, among whom the most important group consists of the so-called pseudoperiodic signals. Pseudoperiodic disturbances may be represented as sums of sinusoidal components, whose frequencies are multiples of some fundamental frequency $\omega_0(t)$

$$s(t) = \sum_{k=1}^{K} a_k(t) e^{j\Sigma_{\tau=0}^{t}\omega_k(\tau)}$$
$$\omega_k(t) = m_k\omega_0(t), \quad k = 1,2,\ldots,K\,. \tag{36}$$

In signal processing, the problem of tracking signals with such a structure is often referred to as the comb filtering problem.

Cancellation of signals governed by (36) may be accomplished using a parallel structure, which consists of multiple SONIC controllers, each tracking and canceling a single harmonic component [53]. Unfortunately, such a solution is hardly efficient, because it does not exploit the relationships between the frequencies of all components. As a result, the subcontrollers in the parallel structure are prone to loosing track of weaker components or switching to different – typically stronger – components.

A novel solution of this problem was presented in papers [57, 58], where a new adaptive comb filtering algorithm was proposed, and its application in active noise control was explained. The new algorithm employs a centralized frequency estimation mechanism, which optimally combines the information carried by all components of the tracked signal. It was shown that the new estimator is a statistically efficient estimator of the fundamental frequency and, via eq. (36), of the frequencies of all harmonic components.

In the case of application in ANC systems, the new algorithm allows one to improve the cancellation performance considerably. Fig. 8 depicts the comparison of power spectral densities of the residual noise from an MRI scanner, resulting from the application of two ANC schemes: standard SONIC algorithm combined with the parallel structure, and the comb variant of the SONIC controller [57]. Poor results obtained using the parallel structure are caused by multiple subcontrollers switching to neighboring, stronger harmonic components. In contrast, the application of the centralized frequency estimation mechanism eliminates this phenomenon completely, which results in unquestionably better controller performance.

5.5 Extension to the multivariate case

The multivariate SONIC controller was proposed in papers [37, 38]. The structure of the controller is close to its univariate version, given in (13). It consists of the inner control loop, whose task is to track and cancel a disturbance, and the outer self-optimization loop, which performs the optimization of the controller's gains. The inner loop has the form

$$\widehat{\mathbf{d}}(t+1|t) = e^{j\omega_0}[\widehat{\mathbf{d}}(t|t-1) + \hat{\mathbf{M}}(t)\mathbf{y}(t)]$$
$$\mathbf{u}(t) = -\mathbf{K}_n^{-1}\widehat{\mathbf{d}}(t+1|t)\,, \tag{37}$$

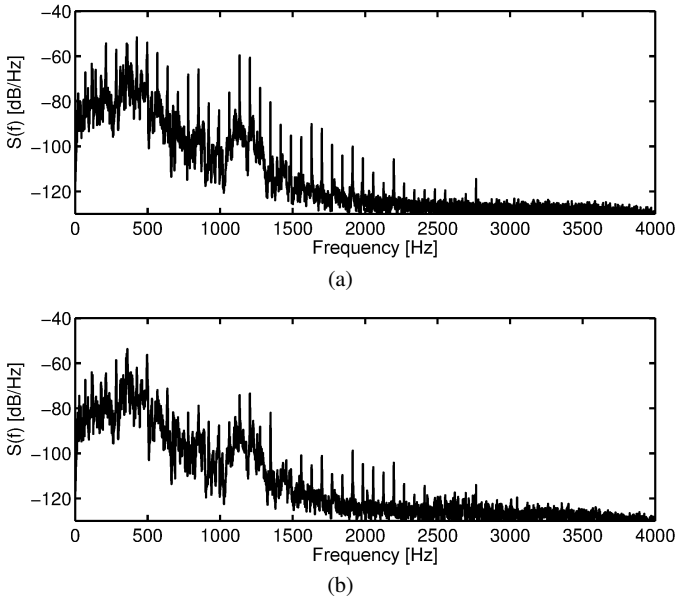

Fig. 8 Comparison of residual MRI noise power spectral densities: (a) Basic SONIC controller. (b) Comb SONIC controller.

where $\widehat{\mathbf{d}}(t+1|t)$ is the one-step prediction of the multivariate disturbance, $\mathbf{u}(t)$ and $\mathbf{y}(t)$ are N-element vectors of control signals and system outputs, respectively, $\mathbf{K}_n$ is the nominal plant gain matrix at frequency ω_0, and $\hat{\mathbf{M}}(t)$ is a complex matrix of adaptation gains, i.e., a multivariate counterpart of the complex gain $\widehat{\mu}(t)$ in algorithm (13).

The outer loop consists of three recursions

$$\begin{aligned}
\tilde{\mathbf{z}}(t) &= e^{j\omega_0}\left[(1-c_\mu)\tilde{\mathbf{z}}(t-1) - c_\mu \mathbf{y}(t-1)\right] \\
\tilde{r}(t) &= \rho\,\tilde{r}(t-1) + |\tilde{\mathbf{z}}(t)|^2 \\
\hat{\mathbf{M}}(t) &= \hat{\mathbf{M}}(t-1)\left[\mathbf{I} - \frac{\mathbf{y}(t)\tilde{\mathbf{z}}^H(t)}{\tilde{r}(t)}\right],
\end{aligned} \tag{38}$$

which, due to the multiplicative gain adjustment mechanism, are a nontrivial extension of the first three equations of the algorithm (13).

The multivariate SONIC controller may undergo further extensions, e.g. to cancel disturbances with unknown frequency, or to employ the hybrid configuration. See [38] for simulated and experimental results illustrating the applications of these concepts in the multivariate case.

5.6 Robustification against impulsive noise

The robustification of the SONIC controller against the adverse effect of impulsive noise was considered in papers [60, 61]. Impulsive noise is typically modeled as heavy-tailed white noise or using α-stable distributions. One may robustifiy the SONIC controller to such noises by replacing the cost criterion (12) with one that employs the L_1 norm

$$V(t;\mu) = \sum_{\tau=1}^{t} \rho^{t-\tau} |y(\tau;\mu)| \,. \tag{39}$$

The study presented in paper [60] shows that the application of the modified cost criterion improves the controller performance in the presence of α-stable measurement noise, $\alpha \in (1,2)$. However, it was observed that the basic variant of the SONIC controller is also quite robust to this kind of disturbances, in the sense that its performance was completely satisfactory from the practical standpoint.

A much more significant challenge than α-stable noises are the disturbances that result from events such as shocks in the walls of an acoustic duct. The presence of such artifacts may cause the SONIC controller to diverge from the optimal settings, or even to destabilize. A suitable modification of the controller, which includes a mechanism that detects such events and freezes the adaptation process until they decay, was proposed in [61]. Typical control results, obtained in real-world acoustic duct using the robust version of the algorithm, are shown in Fig. 9.

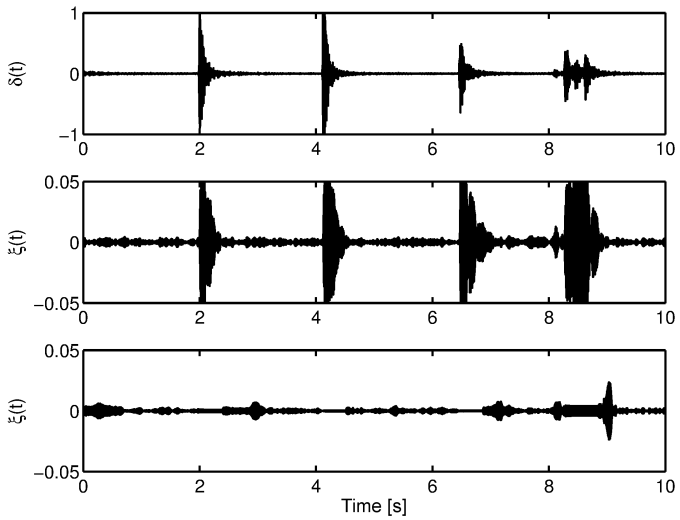

Fig. 9 Comparison of control results obtained using the basic SONIC controller (middle plot) and the robust SONIC controller (bottom plot) in the presence of disturbances caused by mechanical shocks to the acoustic duct (top plot).

References

1. Åström, K.J. *et al.* . Theory and applications of self-tuning regulators. Automatica **13**, 457–476 (1977)
2. Bai, E.-W., Fu, L.-C., Sastry, S.: Averaging analysis for discrete time and sampled data adaptive systems. IEEE Trans. Circuits and Systems **35**, 137–148 (1988)
3. Bodson, M., Douglas, S.C.: Adaptive algorithms for the rejection of sinusoidal disturbances with unknown frequency, Automatica **33**, 2213–2221 (1997)
4. Bodson, M.: Rejection of periodic disturbances of unknown and time-varying frequency, Int. J. Adapt. Control Signal Process. **19**, 67–88 (2005)
5. Van den Bos, A.: Complex gradient and Hessian. IEE Proc. Image Signal Processing **141**, 380–382 (1994).
6. Brandwood, D.H.: A complex gradient operator and its application in array theory. Proc. Inst. Elect. Eng. **130**, 11–16 (1983)
7. Castae-Selga, R., Pea, R.: Active noise hybrid time-varying control for motorcycle helmets. IEEE Trans. Control Syst. Technol. **18**, 602–612 (2010)
8. Chakrovorthy, S.R.: Active snore noise control systems, M.S. Thesis, Northern Illinois University (2005)
9. Chakravarthy, S.; Kuo, S.M.: Application of active noise control for reducing snore, ICASSP 2006, Proc. 2006 International Conference on Acoustics Speech and Signal Procesing, Toulose, France, 305–308 (2006)
10. Chambers, J., Bullock, D., Kahana, Y., Kots, A., Palmer, A.: Developments in active noise control sound systems for magnetic resonance imaging. Appl. Acoust. **68** 281–295 (2007).
11. Chen, C.K., Chiueh, T.T., Chen, J.H.: Active cancellation system of acoustic noise in MR imaging. IEEE Trans. Biomed. Eng. **46**, 186–191 (1999)
12. Crawford, D.H., Stewart, R.W.: Adaptive filtered-V algorithm for active noise control, J. Acoust. Soc. Am. **101**, 2097–2103 (1997)
13. Elliot, S.J., Nelson, P.A.: Active Noise Control. IEEE Signal Process. Mag. **10**, 12–35 (1993)
14. Eriksson, L.J., Allie, M.C., Greiner, R.A.: The selection and application of an IIR adaptive filter for use in active sound attenuation. IEEE Trans. Acoust. Speech Signal Process. **35**, 433–437 (1987)
15. Eriksson, L.J., Allie, M.C.: Use of random noise for on-line transducer modeling in an adaptive active attenuation system, J. Acoust. Soc. Am. **85**, 797-–802 (1989)
16. Eriksson, L.J.: Development of the filtered-U algorithm for active noise control, J. Acoust. Soc. Am. **89**, 257–267 (1991)
17. Engel, Z.: Ochrona środowiska przed drganiami i hałasem. Wydawnictwo Naukowe PWN, Warszawa (2001)
18. Gan, W.S.; Kuo, S.M.: An integrated active noise control headsets. IEEE Trans. Consum. Electron., **48**, 242–247 (2002)
19. Gan, W.S, Mitra, S., Kuo, S.M.: Adaptive feedback active noise control headset: implementation, evaluation and its extensions. IEEE Trans. Consum. Electron. **51**, 975–982 (2005)
20. Guo, X., Bodson, M.: Adaptive rejection of multiple sinusoids of unknown frequency, EUSIPCO 2007, Proc. 2007 European Control Conference, 121–128 (2007)
21. Haykin, S.: Adaptive Filter Theory. Prentice Hall, Englewood Cliffs (1996)
22. Jury, M.: Theory and Application of the $\mathscr{Z}$-transform Method. Wiley, New York (1964)
23. Kajikawa, Y., Gan, W.S., Kuo, S.M.: Recent advances on active noise control: open issues and innovative applications. APSIPA Transactions on Signal and Information Processing, **1**, 1–21 (2012)
24. Kannan, G., Milani, A.A., Panahi, I., Briggs, R.W.: An efficient feedback active noise control algorithm based on reduced-order linear predictive modeling of fMRI acoustic noise. IEEE Trans. Biomed. Eng. **58**, 3303–3309 (2011)
25. Kuo, S.M., Morgan, D.: Active Noise Control Systems: Algorithms and DSP Implementations, Wiley, New York (1995)

26. Kuo, S.M, Gireddy, R.: Real-time experiment of snore active noise control, Proc. 2007 International Conference on Control Applications, Singapore, 1085–1092 (2007)
27. Kuo, S.M., Liu, L., Gujjula, S.:Development and application of audio-integrated active noise control system for infant incubators. J. Noise Control Eng. **58**, 163–175 (2010)
28. Kuo, S.M., Chen, Y.-R., Chang, Ch.-Y., Lai, Ch.-W.: Development and evaluation of lightweight active noise cancellation earphones, Appl. Sciences **8**, 1178 (2018)
29. Landau, L.D., Constantinescu, A., Rey, D.: Adaptive narrow band disturbance rejection applied to an active suspension - an internal model principle approach, Automatica **41**, 563–574 (2005)
30. Liu, L.C., Kuo, S.M., Raghuathan, K.: An audio integrated motorcycle helmet. J. Low Freq. Noise Vib. Active Control **29**, 161–170 (2010)
31. Liu, L., Du, L., Kolla, A.: Wireless communication integrated hybrid active noise control system for infant incubators. Proc. 2016 IEEE Signal Processing in Medicine and Biology Symposium, Philadelphia, USA, 1–6 (2016)
32. Manolakis, D.G., Ingle, V.K., Kogon, S.M.: Statistical and adaptive signal processing: spectral estimation, signal modeling, adaptive filtering, and array processing. Boston: McGraw-Hill (2000)
33. Nelson, P.A., Elliot, S.J.: Active Control of Sound, Academic Press, London (1993)
34. Meller, M.: Samooptymalizujące adaptacyjne tłumienie zakłóceń wąskopasmowych. Rozprawa doktorska, Politechnika Gdańska, Wydział Elektroniki, Telekomunikacji i Informatyki (2010).
35. Meller M., Niedźwiecki, M.: Robustification of the self-optimizing narrowband interference canceller - extremum seeking in complex domain. CDC 2012, Proc. 51st IEEE Conference on Decision and Control, Maui, Hawaii, USA, 4805–4810 (2012)
36. Meller, M., Niedźwiecki, M.: Parallel frequency tracking with built-in performance evaluation. Digital Signal Process., vol. 32, pp. 845-851, 2013.
37. Meller M., Niedźwiecki, M.: Multiple-channel frequency-adaptive active vibration control using SONIC. ISPA 2013, Proc. 8th International Symposium on Image and Signal Processing and Analysis, Trieste, Italy, 620–625 (2013).
38. Meller, M., Niedźwiecki, M.: Multichannel self-optimizing narrowband interference canceller. Signal Process. **98**, 396–409 (2014)
39. Morgan, D.R.: An analysis of multiple correlation cancellation loops with a filter in the auxiliary path. IEEE Trans. Acoust. Speech Signal Process. **28**, 454–467 (1980)
40. Nehorai, A.: A minimal parameter adaptive notch filter with constrained poles and zeros. IEEE Trans. Acoust, Speech Signal Process. **33**, 983–996 (1985)
41. Niedźwiecki, M.: Steady state and parameter tracking properties of self-tuning minimum variance regulators. Automatica **25**, 597–602 (1989)
42. Niedźwiecki, M.: Identification of Time-varying Processes. Wiley, New York (2000)
43. Niedźwiecki, M., Kaczmarek, P.: Generalized adaptive notch and comb filters for identification of quasi-periodically varying system. IEEE Transactions on Signal Processing **53**, 4599–4609 (2005)
44. Niedźwiecki, M., Kaczmarek, P.: Tracking analysis of a generalized adaptive notch filter. IEEE Transactions on Signal Processing **54**, 304–314 (2006)
45. Niedźwiecki, M., Sobociński, A.: A simple way of increasing estimation accuracy of generalized adaptive notch filters. IEEE Signal Processing Letters **14**, 217–220 (2007)
46. Niedźwiecki, M.: Adaptive notch smoothing revisited. EUSIPCO 2008, Proc. 16th European Signal Processing Conference, Lausanne, Switzerland, 1–5 (2008)
47. Niedźwiecki, M., Meller, M.: A new a pproach to active noise and vibration control – Part I: the known frequency case. IEEE Transactions on Signal Processing **57**, 3373–3386 (2009)
48. Niedźwiecki, M., Meller, M.: A new a pproach to active noise and vibration control – Part II: the unknown frequency case. IEEE Transactions on Signal Processing **57**, 3387–3398 (2009)
49. Niedźwiecki, M., Meller, M.: Self-optimizing adaptive vibration controller. IEEE Transactions on Automatic Control **54**, 2087–2099 (2009)

50. Niedźwiecki, M., Meller, M.: Self-optimizing scheme for active noise and vibration control. ICASSP 2009, Proc. 2009 IEEE International Conference on Acoustics, Speech and Signal Processing, Taipei, Taiwan, 249–252 (2009)
51. Niedźwiecki, M., Meller, M.: An improved frequency estimator for an adaptive active noise control scheme. EUSIPCO 2010, Proc. 18th European Signal Processing Conference, Aalborg, Denmark, 353–357 (2010)
52. Niedźwiecki, M.: Generalized adaptive notch smoothing revisited. IEEE Transactions on Signal Processing **58**, 1565–1576 (2010)
53. Niedźwiecki, M., Meller, M.: Multifrequency self-optimizing narrowband interference canceller. IWAENC 2010, Proc. 18th International Workshop on Acoustic Echo and Noise Control, Tel Aviv, Israel, 1–4 (2010).
54. Niedźwiecki, M., Meller, M.: SONIC – Self-optimizing narrowband interference canceler: comparison of two frequency tracking strategies. Proc. 8th IEEE International Conference on Control and Automation, Xiamen, China, 1892–1896 (2010)
55. Niedźwiecki, M., Meller, M.: New algorithms for adaptive notch smoothing. IEEE Transactions on Signal Processing **59**, 2024–2037 (2011)
56. Niedźwiecki, M., Meller, M.: Generalized adaptive comb filter with improved accuracy and robustness properties. EUSIPCO 2012, Proc. 20th European Signal Processing Conference, Bucharest, Romania 91–95 (2012)
57. Niedźwiecki M., Meller, M., Kajikawa, Y., Łukwiński, D.: Estimation of nonstationary harmonic signals and its application to active control of MRI noise. ICASSP 2013, Proc. 2013 IEEE International Conference on Acoustics, Speech and Signal Processing, Vancouver, Canada, 5661–5665 (2013)
58. Niedźwiecki, M., Meller, M.: Generalized adaptive comb filters/smoothers and their application to the identification of quasi-periodically varying systems and signals. Automatica **49**, 1601–1613 (2013).
59. Niedźwiecki, M., Meller, M.: Hybrid SONIC: joint feedforward-feedback narrowband interference canceller. Int. Journ. Adaptive Contr. and Signal Process. **27**, 1048–1064 (2013).
60. Niedźwiecki M., Meller, M.: Robust algorithm for active feedback control of narrowband noise. EUSIPCO 2015, Proc. 23rd European Signal Processing Conference, Nice, France, 275–279 (2015)
61. Niedźwiecki M., Meller, M.: Active feedback noise control in the presence of impulsive disturbances. ICASSP 2015, Proc. 2015 IEEE International Conference on Acoustics, Speech and Signal Processing, Brisbane, Australia, 659–663 (2015)
62. Panahi, I.M.S.: Development of ANC methods for fMRI rooms: Design challenges and algorithms, Proc. 2013 International Symposium on Image and Signal Processing and Analysis, Trieste, Italy, 655-660 (2013)
63. Raghunathan, K., Kuo, S.M., Gan, W.S.: Active noise control for motorcycle helmets, in Proc 2010 International Conference on Green Circuits and Systems, Shanghai, China, 170–174 (2010)
64. Regalia, P.A.: An improved lattice-based adaptive IIR notch filter. IEEE Trans. Signal Process. 39, 2124–2128 (1991)
65. Roy, R.,Kailath, T.: ESPRIT – Estimation of Signal Parameters via Rotational Invariance Techniques, IEEE Trans. Acoust. Speech Signal Process. **37**, 984–995 (1989)
66. Schimidt, R.O.: Multiple Emiter Location and Signal Parameter Estimation, IEEE Trans. Antenn. Propag. **34**, 276–280 (1986)
67. Silva A.C., Landau, I.D., Airimitoaie, T-B.: Direct adaptive rejection of unknown time-varying narrow band disturbances applied to a benchmark problem, Eur. J. Control **19**, 326–336 (2013)
68. Skogestad, S., Postlethwaite, I.: Multivariate Feedback Control: Analysis and Design. Wiley, New York (2005)
69. Söderström, T., Stoica, P.: System Identification. Prentice Hall, Englewood Cliffs, New Jersey (1988)

70. Takar, M.S., Kumar Sharma, M., Pal, R.: A review on evolution of acoustic noise reduction in MRI. Proc 2017 Recent Developments in Control, Automation Power Engineering, Noida, India, 235–240 (2017)
71. Tichavský, P., Händel, P.: Two algorithms for adaptive retrieval of slowly time-varying multiple cisoids in noise. IEEE Trans. Signal Process. **43**, 1116–1127 (1995)
72. Tichavský, P.: Posterior Cramér-Rao bound for adaptive harmonic retrieval. IEEE Trans. Signal Process. **43**, 1299–1302 (1995)
73. van Trees. H.L., Bell K.L., Tian, Z.: Detection, Estimation and Modulation Theory, Part I: Detection, Estimation, and Filtering Theory, Wiley, New York (2013)
74. Wang, T.W., Gan, W.S., Kuo, S.M.: Subband-based active noise equalizer for motorcycle helmets, Proc. 2010 ASIPA ASC 2010, Singapore, 555-559 (2010)
75. Widrow, B., Stearns, S.D.: Adaptive Signal Processing, Prentice-Hall, Englewood Cliffs (1985)
76. Wirtinger, W.: Zur formalen theorie der funktionen von mehr komplexen veränderlichen. Math. Ann. **97**, 357–375 (1927)
77. Yu, X., Gujjula, S., Kuo, S.M.:Active noise control for infant incubators. Proc. 2009 Annual International Conference of the IEEE Engineering in Medicine and Biology Society, Minneapolis, USA, 2531–2534 (2009)

Index